Multiphase materials with lignin: 13. Block copolymers with cellulose propionate

Willer de Oliveira and Wolfgang G. Glasser*
Department of Wood Science and Forest Products, and Biobased Materials Center, Virginia Tech, Blacksburg, Virginia 24061, USA
(Received 21 June 1993; revised 13 September 1993)

Block copolymers consisting of rubbery lignin derivative components (i.e. hydroxypropyl lignin, L) and cellulose propionate (CP) segments ranging in size from degree of polymerization (*DP*) 5 to 60 were synthesized using chemistry described previously. The block copolymers (LCP) varied in relation to architecture and size of component. The copolymers were characterized by solution, thermal and optical techniques, and their effect on the properties of L/CP blends was determined by mechanical tests. The results suggest that copolymer properties are dictated primarily by CP segment size. Whereas copolymers with short CP segments behaved like spherical macromolecules, copolymers with large CP segments had rod-like behaviour. All block copolymers displayed T_m values, even if CP arm length was as low as 5. Crystallinity was highest at CP chains of *DP* 60. Copolymer morphologies varied; they revealed patterns resembling dispersed fibrils, spheres and alternating lamella types depending on composition and segment geometries. The block copolymers had surprisingly little effect on L/CP blend properties. This was attributed to the overall compatibility of lignin derivatives with CP.

(Keywords: lignin; block copolymers; cellulose propionate)

INTRODUCTION

The synthesis of multiphase block copolymers with thermoplastic processability has been the subject of extensive research. However, only a few successful approaches have been reported on the synthesis of cellulose-containing block copolymers[1,2]. One of the earliest methods to produce block copolymers containing cellulose was based on the mastication technique of high-molecular-weight cellulose derivatives in the presence of polymerizable monomers. The formation of polymeric free radicals by the main-chain scission of the cellulose backbone was the key step to the initiation of (block) copolymerization. Methyl cellulose–acrylonitrile copolymers as well as ethyl cellulose–methyl methacrylate and bemzyl cellulose–styrene copolymers were produced by this technique[1].

A different approach to the synthesis of cellulose-containing block copolymers was employed by Steinmann[2]. Segmented multiblock copolymers were produced from dihydroxy-terminated cellulose triacetate segments and low-molecular-weight polyesters or polyethers that were end-capped with isocyanate groups. Stannett, Gilbert and associates[3–5] advanced the synthesis procedure for the purpose of producing a new class of biodegradable polymers. Their goals were to remove the hydroxy-blocking acetyl groups on the cellulose triacetate blocks to produce another kind of block copolymer, one with biodegradable properties.

A major problem with these synthesis techniques was the generation of considerable chain branching, grafting or crosslinking. By using a long-known carbohydrate reaction[6], Cantow *et al.*[7,8] produced a fully substituted cellulose derivative by acidolytic cleavage that was monofunctional. This oligomeric cellulose derivative could be used as a prepolymer for the synthesis of block copolymers. Monohydroxy-terminated cellulose derivatives were coupled with 4,4′-dithiodi-(phenylisocyanate) and then used as a macrophotoinitiator for radical three-block copolymer synthesis. Polymerizations were performed by irradiating solutions of the macroinitiators in mixtures of the monomers styrene, chloroprene and methacrylate. Copolymers with high rubber-like elasticity in connection with thermoplastic processability were obtained.

In a recent publication, the preparation and properties of monofunctional cellulose propionate segments have been described[9]. It has also been reported that hydroxypropyl lignin (L) can be synthesized with variable thermal properties, with either glassy or rubbery behaviour[10,11]. The purpose of this paper is to study the synthesis of multiphase star-like copolymers (LCP) between low-molecular-weight L and semicrystalline, monofunctional cellulose propionate (CP) oligomers. The main aim is to analyse the influence of CP segment size and L molecular weight on the solution and thermal behaviour, and on the morphological features of the copolymers; and to examine the properties of melt-blended L/CP materials before and after the addition of LCP copolymer as blend compatibilizer.

EXPERIMENTAL MATERIALS

Cellulose propionate (CP)

Commercial cellulose propionate was purchased from Aldrich Chemical Co. It was used as received.

*To whom correspondence should be addressed

0032-3861/94/09/1977–09

Monohydroxy-terminated CP segments

Monohydroxy-functional CP segments were obtained by hydrolysis of CP in accordance with an earlier publication[9]. CP segments ranged in size (M_n) from 1600 to 18 500 g mol^{-1}, and they had molecular-weight distributions (M_w/M_n) of 1.2 to 1.8.

Hydroxypropyl lignin (L)

L with variable molecular weight and molecular-weight distribution was obtained by propoxylating Kraft and Organosolv lignins in accordance with earlier publications[10,11]. All lignin derivatives used had degrees of modification with propylene oxide which, after solvent fractionation, resulted in copolymers with different sizes and glass transition temperatures, T_g, below room temperature (see *Table 1* for descriptions). For the blend study, two types of L were used. The lesser propoxylated lignin, L(A) (M_n of 1900) had its T_g above room temperature (84°C), and was obtained from a commercial Kraft lignin (Indulin AT, Westvaco Corp.); the more highly propoxylated lignin, L(B) (M_n of 10000) had its T_g below room temperature (−7°C) and was prepared by reaction of Organosolv (aqueous ethanol) lignin from aspen with propylene oxide.

Others

2,4-Tolylene diisocyanate (TDI), stannous octanoate and tetrahydrofuran (THF) were purchased from Aldrich Chemical Co. and used without further purification, except THF, which was dried over metallic potassium and benzophenone mixture, refluxed and distilled under dried nitrogen.

METHODS

Synthesis of monoisocyanate-terminated CP segment

In a typical synthesis of monoisocyanate-terminated cellulose propionate segments (CP-NCO), 1 g of CP and 0.1% by weight of stannous octanoate were introduced into a two-necked flask equipped with a magnetic stir bar. The flask was connected to a vacuum line for further drying. After 6 h, the reactor was sealed with rubber septa, transferred to an oil bath on a stir plate and purged with prepurified and dried nitrogen. Under a constant flow of nitrogen, 10 ml of freshly distilled THF were added into the reaction flask through a hypodermic syringe to dissolve the reactants. The reactor was heated to 50°C and then TDI was added in an approximately 5:1 molar ratio. The reaction was kept at 50°C under stirring for 24 h. After cooling, the product was precipitated into a large excess of petroleum ether to eliminate unreacted TDI, filtered, washed with petroleum ether and dried under vacuum. The monoisocyanate-capped prepolymer was immediately used for grafting. Infra-red spectroscopy was used to monitor the reaction.

Copolymer synthesis

The grafting of NCO-functional segments onto OH-functional lignin derivatives was performed in a clean, flamed, nitrogen-purged two-necked round-bottomed flask equipped with a magnetic stir bar and rubber septa under prepurified and dried nitrogen atmosphere. First, a calculated amount of L and stannous octanoate dissolved in THF were charged to the reaction flask through a hypodermic syringe. Next, CP-NCO dissolved in THF was syringed into the flask at a 2:1 molar ratio of CP-NCO to L. The reaction flask was submerged into the oil bath and heated to 50°C. The grafting reaction was terminated after 24 to 30 h through precipitation into aqueous methanol. The copolymer was collected by filtration and drying in a vacuum desiccator. Unincorporated L was removed by Soxhlet extraction with methanol.

Characterization

Molecular parameters. Molecular weights, Mark–Houwink–Sakurada constants and intrinsic viscosities were determined by gel permeation chromatography in THF using sequential detection with a refractive index and a differential viscosity detector in accordance with a method described previously[12].

Spectroscopic characterization. *FT*-i.r. spectra were recorded using a Nicolet 5SX spectrophotometer; samples were prepared by dispersion in KBr. U.v. spectra were recorded in chloroform solution using a Varian/Cary-219 UV-VIS spectrophotometer.

Thermal analysis. D.s.c. thermograms were obtained on a Perkin–Elmer model DSC-4 instrument equipped with a thermal analysis data station. Temperature was scanned from −60 to 300°C at a heating rate of 10°C min^{-1}. The scanning procedure involved two runs through T_m with quenching to −60°C following the first scan. Glass transition temperatures (T_g) were taken as mid-points of the change in slope of the baseline. T_m was taken as the temperature corresponding to the location of the melt endotherm.

Dynamic thermal analysis (d.m.t.a.) was conducted using a Polymer Laboratories Ltd d.m.t.a. instrument. Injection-moulded samples were scanned from −50°C through T_g at a heating rate of 10°C min^{-1} and a frequency of 1 Hz.

Microscopy. Optical microscopy was conducted on a Zeiss Axioplan microscope fitted with a Linkam TMS90 hot stage and a Zeiss ML 100 camera. Nucleation behaviour and crystal growth were observed on thin films of copolymers between glass plates.

Tensile test. All mechanical tests were performed on dog-bone specimens using a floor model Instron instrument at a cross-head speed of 0.25 inch/min (~6.3 mm min^{-1}). Each value represents the average of four to seven tests.

Transmission electron microscopy. TEM was carried out on a Phillips EM-420 STEM operated in the transmission mode at 10 kV. Ultrathin films were microtomed using a Reichert-Jung Ultracut System FC-4 at −70°C. The microtomed samples were then mounted on a copper TEM grid and stained with RuO_4 for 15–45 min.

Blend preparation

Blends of CP, L and (optional) LCP copolymer were prepared in a Custom Scientific Instrument (CSI) melt extruder. The extrudate was chopped and subsequently injection moulded into dog-bone test specimens. The procedure has been described previously[13]. The extrusion temperature was 200°C, and the residence time was no longer than 2 min. Several blend combinations could not be prepared by melt extrusion owing to viscosity

incompatibility: this condition was recognized by macroscopic separation of L from CP whereby the lower-viscosity L component served to lubricate the injector barrel and physically separated from CP. This prevented the melt mixture from passing through the orifice into the mould.

RESULTS AND DISCUSSION

Copolymer synthesis

A series of LCP copolymers was synthesized by coupling monofunctional CP segments to OH-functional L segments using urethane chemistry. The resulting copolymers contained L as the elastomeric centre block while the terminal blocks represented CP. The synthesis of these copolymers followed earlier work developed for L copolymers with caprolactone[14,15].

Copolymer stoichiometry was kept constant, with an average of two arms per M_n-average core segment. The course of the grafting reaction using NCO-functional CP segments was followed by *FT*-i.r. spectroscopy using the NCO absorption peak at 2274 cm^{-1} for grafting diagnosis. In addition, copolymer characterization involved gel permeation chromatography (*Figure 1*). The characteristically narrowly dispersed CP segments formed broader distributions following attachment to the typically broadly dispersed L component. Depending on overall L content, the resulting copolymer distribution resembled either the CP or the L parent segment (*Figure 1a* vs. *1b*, respectively). The extent to which the reaction product consisted of copolymer as opposed to unreacted parent segments was judged on the basis of (a) the total removal of unreacted L by Soxhlet extraction (5 to 15% by weight) and (b) the analysis of the g.p.c. chromatogram of the copolymer. No peak was apparent at the molecular weight of the CP oligomer, and this is an indication of the non-existence of unreacted CP oligomers mixed with the copolymer.

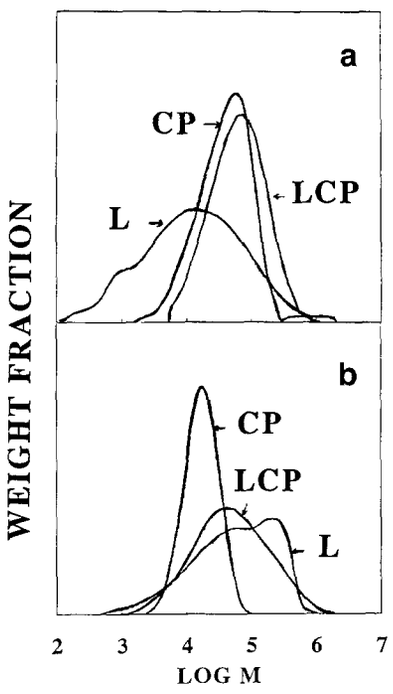

Figure 1 Typical molecular-weight distribution of LCP copolymers (and their corresponding prepolymers) with (a) high CP content and (b) high L content

A third method of copolymer characterization involved u.v. spectroscopy. Since lignin was the only u.v.-absorbing component in the copolymer consisting of CP, propylene oxide and lignin, u.v. absorption measurements allowed the quantitative determination of lignin content.

The block copolymers produced made use of combinations of CP and L segments in different proportions (*Table 1*). Copolymers ranged in molecular weight (M_n) between 4000 and 30 000, in lignin content between 5 and 45%, in L segment size between 1800 and 6900 g mol^{-1}, and in CP segment size between DP_n 5 and 60 (i.e. 1600 to 18 500 g mol^{-1}).

Solution properties

Block copolymers, especially those with star-like architecture, have solution properties typical of spherical molecules. Cellulosic (arm) segments, by contrast, retain the rod-like conformation typical of cellulose derivatives. Combinations of CP and L take on hybrid character in which the properties typical of either one of the two parents dominate. The relationship between CP arm length and intrinsic viscosity (*IV*) for a variety of block copolymer types revealed a steady increase in log *IV* when both arm length and core size rose (*Figure 2b*); but a distinct step-wise transition was detected for the copolymers in which the length of the CP segment exceeded the size of the (invariable) L core by a factor of 2 or 3 (*Figure 2a*). This sudden rise in viscosity at CP segment M_n of about 6000 suggests a change in copolymer conformation from spherical to rod-like. In agreement with the results obtained for hydroxypropyl lignin–polycaprolactone block copolymers reported earlier[15], the intrinsic viscosities of the LCP copolymers with short arm length were higher than the linear CP segments of equivalent molecular weight (*Figure 2a*). This may be related to an increased incompatibility between segments as a result of the incorporation of urethane groups after the capping reaction with TDI.

The relationship between the Mark–Houwink–Sakaruda (MHS) exponential factor *a* and CP arm length indicated that *a* rose steeply with increasing arm length before reaching a plateau when the arm length corresponded to the size of the central core (*Figure 2b*). This suggests that the copolymers with short arm length behave in solution like spherical, flexible polymer molecules, whereas high-molecular-weight copolymers with long arms assume a rod-like conformation (in solution).

Thermal properties

A typical d.s.c. thermogram of LCP exhibited a melt endotherm peak for the CP chains at 230–240°C; two glass transition temperatures representing the amorphous phases of L and CP located between −40 and −10°C and at 130°C, respectively; and a crystallization temperature at 160°C (*Figure 3*). The thermogram provides strong evidence for phase separation of L from the CP hard segments. The thermal data of LCP copolymers are summarized in *Table 2* on the basis of their CP arm length. Even at *DP* 5, it was possible to detect the formation of a small endotherm at 190°C, which is an indication of the crystallization of CP chains. As the molecular weights of the CP arm segments increased, the major melt endotherm was observed at increasingly higher temperatures, levelling off at a *DP* of approximately 50 and a T_m of about 240°C. Although not prominent

Table 1 Characteristics of copolymer and blend components

Sample	CP					L				Copolymer			
	$M_n \times 10^3$	DP_n	M_w/M_n	a^a	IV^b	$M_n \times 10^3$	M_w/M_n	a	IV	$M_n \times 10^3$	M_w/M_n	a	IV
Blend components													
CP[c]	120.0	382	1.6	0.80	1.80	–	–	–	–	–	–	–	–
L(A)[d]	–	–	–	–	–	1.9	6.3	0.20	0.04	–	–	–	–
L(B)[e]	–	–	–	–	–	10.0	5.2	0.24	0.08	–	–	–	–
Copolymer components[f]													
F1	1.6	5	1.2	0.53	0.03	3.0	5.1	0.16	0.11	4.1	3.5	0.23	0.08
F2	3.9	12	1.4	0.80	0.03	1.8	10.5	0.17	0.06	4.8	2.1	0.46	0.08
F3	5.0	16	1.6	0.78	0.09	2.1	7.5	0.20	0.11	8.2	1.3	0.54	0.18
F4	11.8	38	1.5	0.91	0.20	2.1	7.5	0.20	0.11	19.3	1.8	0.87	0.29
F5	12.6	40	1.4	0.94	0.20	6.9	8.9	0.26	0.11	18.9	6.2	0.86	0.12
F6	18.5	59	1.8	0.96	0.48	1.8	10.5	0.17	0.06	28.4	1.7	0.79	0.45
F7	18.5	59	1.8	0.96	0.48	1.8	10.5	0.17	0.06	27.0	1.8	0.92	0.45
F8	18.5	59	1.8	0.96	0.48	1.8	10.5	0.17	0.06	24.6	2.1	0.60	0.45

[a] Mark–Houwink–Sakurada exponential constant
[b] Intrinsic viscosity ($dl\,g^{-1}$)
[c] Cellulose propionate purchased from Aldrich Chemical Co.
[d] Hydroxypropyl lignin obtained from Kraft lignin (Indulin AT, Westvaco Corp.)
[e] Hydroxypropyl lignin obtained from Organosolv lignin (Aldrich Chemical Co.)
[f] The different sizes of the L and CP segments in the LCP copolymer series were produced by solvent fractionation of Organosolv lignin and hydrolysis of high-molecular-weight cellulose propionate, respectively (Aldrich Chemical Co.)

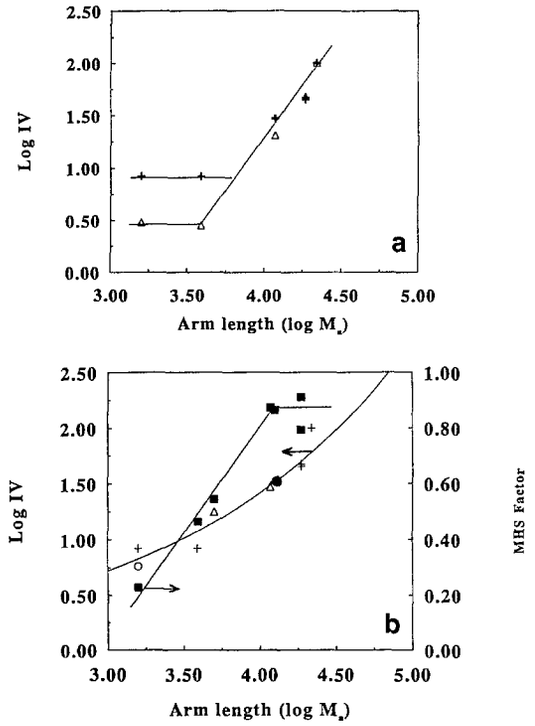

Figure 2 Intrinsic viscosity and Mark–Houwink–Sakurada exponential factor as functions of CP arm length for LCP copolymers: (a) copolymers with L of constant molecular weight (1800) (+) and their respective CP segments only (△); (b) copolymers with L of different molecular weights: 1800 (+), 2100 (○), 3000 (△) and 6900 g mol^{-1} (●) and their MHS factors (■)

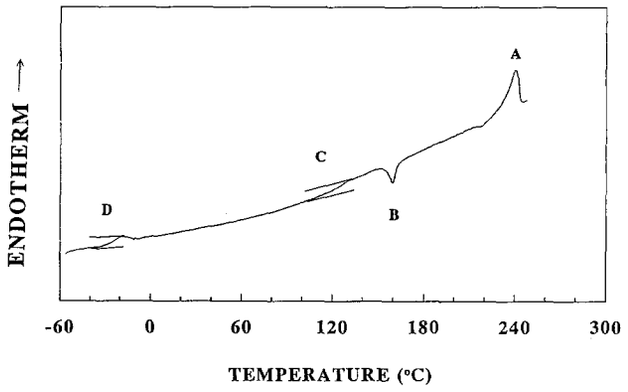

Figure 3 Typical d.s.c. thermogram of LCP copolymer quenched from the melt. A, B and C are the melting, crystallization and glass transition temperatures of CP blocks, whereas D is the glass transition temperature of the L phase. Heating rate: 10°C min^{-1}

Table 2 Summary of thermal data of LCP copolymers

Sample	M_n/arm	T_g(L) (°C)	T_g(CP) (°C)	T_m(CP) (°C)	ΔH_f ($J\,g^{-1}$)
F1	1 600	−32	110	190	<1
F2	3 900	−19	117	205	2
F3	5 000	−23	125	226	31
F4	11 800	−25	130	224	31
F5	12 600	−15	120	223	35
F6	18 500	−20	118	239	54
F7	18 500	−28	121	237	63
F8	18 500	−30	130	238	72

on the second scan, the majority of the copolymers presented in this work revealed glass transition temperatures for L and CP during the initial d.s.c. scans.

The d.m.t.a. spectrum of a high-molecular-weight LCP copolymer revealed three major thermal events, and these were a T_g of L at around 0°C, a T_g of the CP component (124°C) and a CP melting point at about 230°C (*Figure 4*). Upon passing through the T_g of the cellulose propionate hard segment, a striking rise in storage modulus was recorded. This signifies a thermally induced organization of the amorphous cellulose derivative chains into a new, ordered (crystalline) morphology.

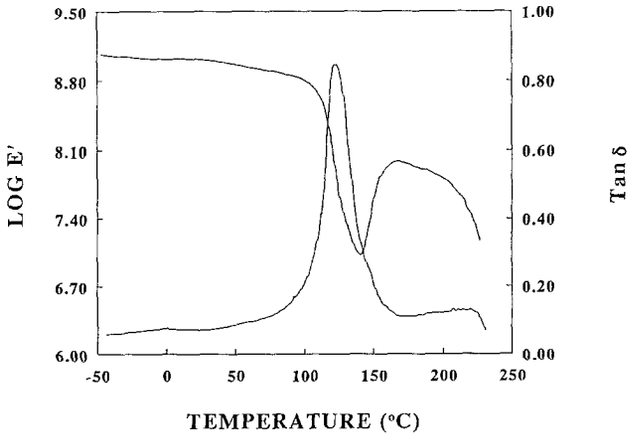

Figure 4 Storage modulus and loss tangent behaviours of typical LCP copolymer

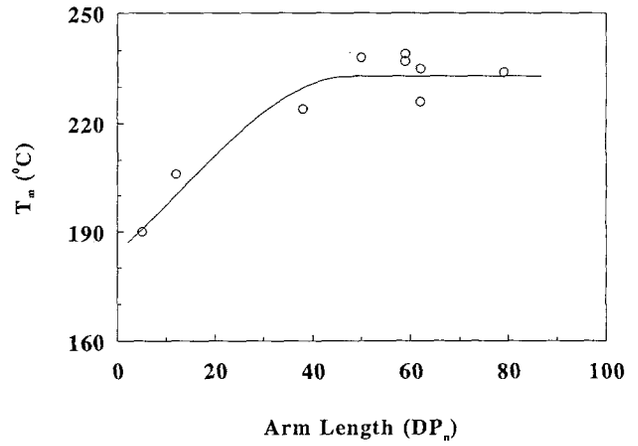

Figure 5 The effect of CP segment size (arm length) on the melting temperature of LCP copolymers

The relationship between melting temperature and arm length showed that, as the copolymer arm length increased, the T_m asymptotically approached a constant temperature level of about 240°C (*Figure 5*). Thus, it can be concluded that, as the arm length increases, a higher degree of phase separation between L and CP is achieved, and more perfect crystallites are produced, as suggested by the higher melting points.

The relationship between heat of fusion ΔH_f, and copolymer arm length indicated that, as the CP chain length increased, ΔH_f increased, and so did crystallinity, which reached its highest content at DP_n around 60 (*Table 2*).

Morphology

Optical micrographs of films isothermally crystallized from the melt at 220°C are shown in *Figure 6*. The micrographs revealed that the crystallized films were spherulitic in texture, but that their size varied. Both copolymer types had the same size L segment, but they differed in CP segment size. Small and homogeneous spherulites with sizes averaging 50 μm were produced by sample with CP segment size 5000 (*Figure 6a*). As the CP segment molecular weight increases, the size of the spherulites decreases by more than an order of magnitude (*Figure 6b*).

Electron micrographs of thin films of LCP cast from dilute solution in THF indicated a broad variety of features (*Figures 7–9*). The dark regions are the L segments selectively stained with ruthenium tetroxide. They varied from dispersed fibrils in copolymers with short arm length (*Figure 7*) to alternate lamellae type of arrangements (*Figure 9*) in copolymers in which both CP and L have high molecular weights. Each figure is composed of a set of micrographs of different magnification for a particular block copolymer (see *Table 1* for sample identification).

The electron micrographs of sample F3, with CP segments of 5000 g mol^{-1} corresponding to a DP_n of 16 and representing a L content of 25%, demonstrated structural organization with fine, dispersed fibrils (*Figure 7*). Average filament length varied between 1000 and 2000 Å, and width was approximately 100 Å. This type of morphology is not uncommon for cellulose derivatives. Buleon and Chanzy[16] have prepared cellulose II crystals through homogeneous deacetylation of cellulose triacetate of *DP* 15 from dilute aqueous solution. Ribbon-like lamellar single crystals were formed with a length of between 1 and 2 μm, a width of approximately 1000 Å and a thickness of around 80 Å. They were characterized by TEM and electron diffraction. They support the opinion that the cellulose molecular axis is perpendicular to the length of the ribbon. Chain folding does not adequately describe the crystallization mechanism since only low-molecular-weight cellulose samples were used.

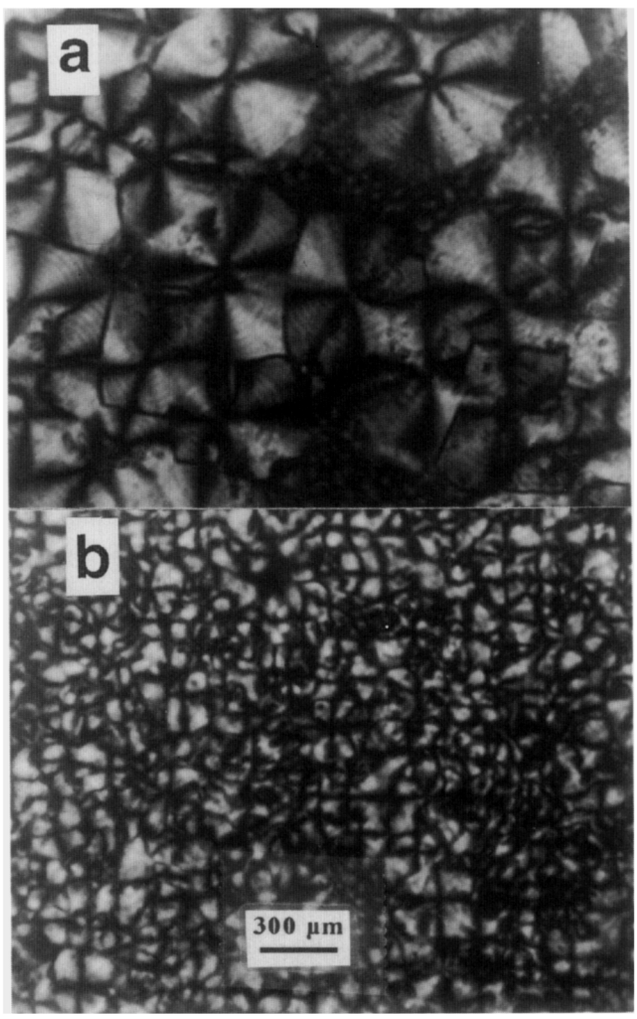

Figure 6 Optical micrographs of films isothermally crystallized from the melt of LCP copolymers with variable CP length (polarized light): (a) CP of DP_n 16; (b) CP of DP_n 38

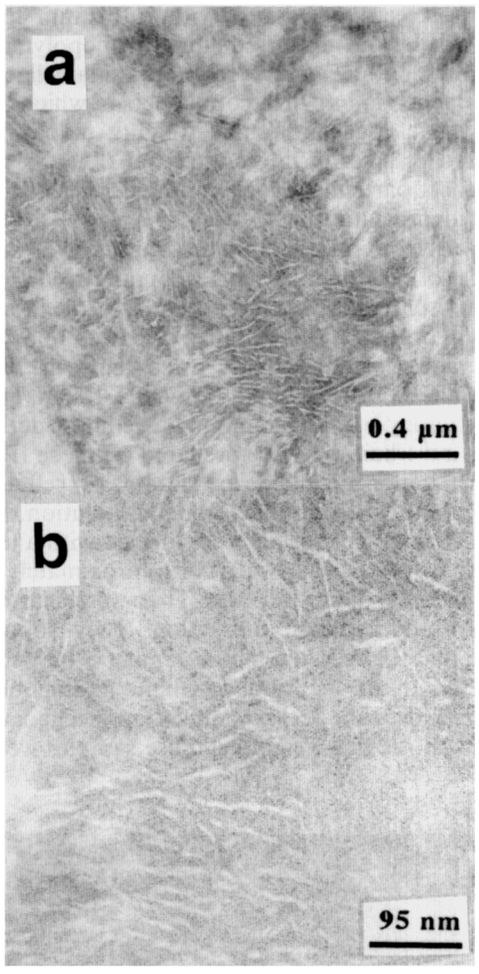

Figure 7 Transmission electron micrographs for cast films of LCP copolymer (F3) seen at different levels of magnification: (a) 37 500×; (b) 105 000×. L phase (dark area) was selectively stained with ruthenium tetroxide. See *Table 1* for sample identification

The filament widths presented here varied between 100 and 300 Å; this is much smaller than the widths of the needle-like structures reported by Buleon and Chanzy. Even though no electron diffraction has been used to characterize these crystals further, it seems that the cellulose propionate chains crystallize in their fully extended form.

The electron micrographs of sample F4, with CP arm length of M_n 11 800 and L size of M_n 6100, presented evidence of almost spherical L particles (stained black), which were dispersed evenly in the CP matrix (*Figure 8*). The dimensions of the particles varied from 200 to 300 Å, and they were not always separated from each other.

The micrographs of *Figure 9* showed very different configurations from the previous samples. Differently from *Figure 8*, the features did not reveal spherical domains. The copolymers segregated into two phases, mostly in the form of alternate layered structures of L and CP. Roughly, the dimensions of the CP layers varied between 100 and 500 Å in width and 2000 to 7000 Å in lamella length. The spacing measurements were obtained by averaging the values across several sets of lines in the micrograph. It is interesting to note that the width of the cellulose propionate layers was equivalent to approximately twice that of a fully extended CP chain.

Blend properties

Block copolymers are often employed as morphology control agents for blends consisting of incompatible polymer components. Block copolymers between L and CP therefore can be examined as additives to blends of L with CP. Blend properties, determined by overall morphology, can be examined by thermal, mechanical and optical techniques. In this study, blends of L with CP were prepared by melt processing techniques in which the L component had either a T_g above (L(A)) or below (L(B)) ambient (*Table 1*). These blends were prepared with

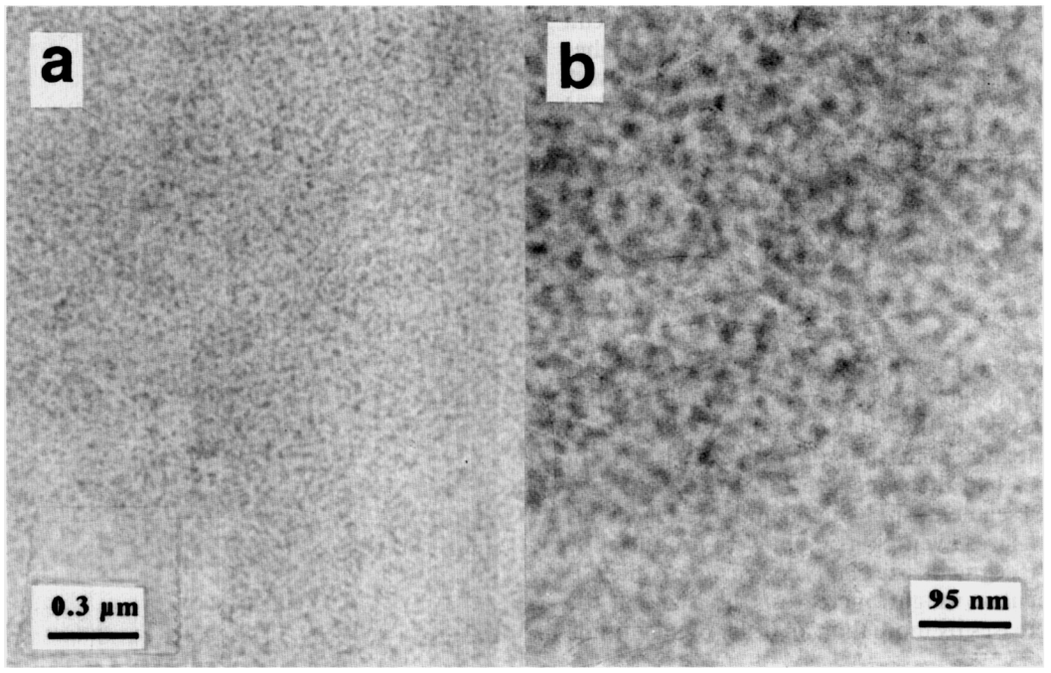

Figure 8 Transmission electron micrographs for cast films of LCP copolymer (F4) seen at different levels of magnification: (a) 37 500×; (b) 105 000×. L phase (dark area) was selectively stained with ruthenium tetroxide. See *Table 1* for sample identification.

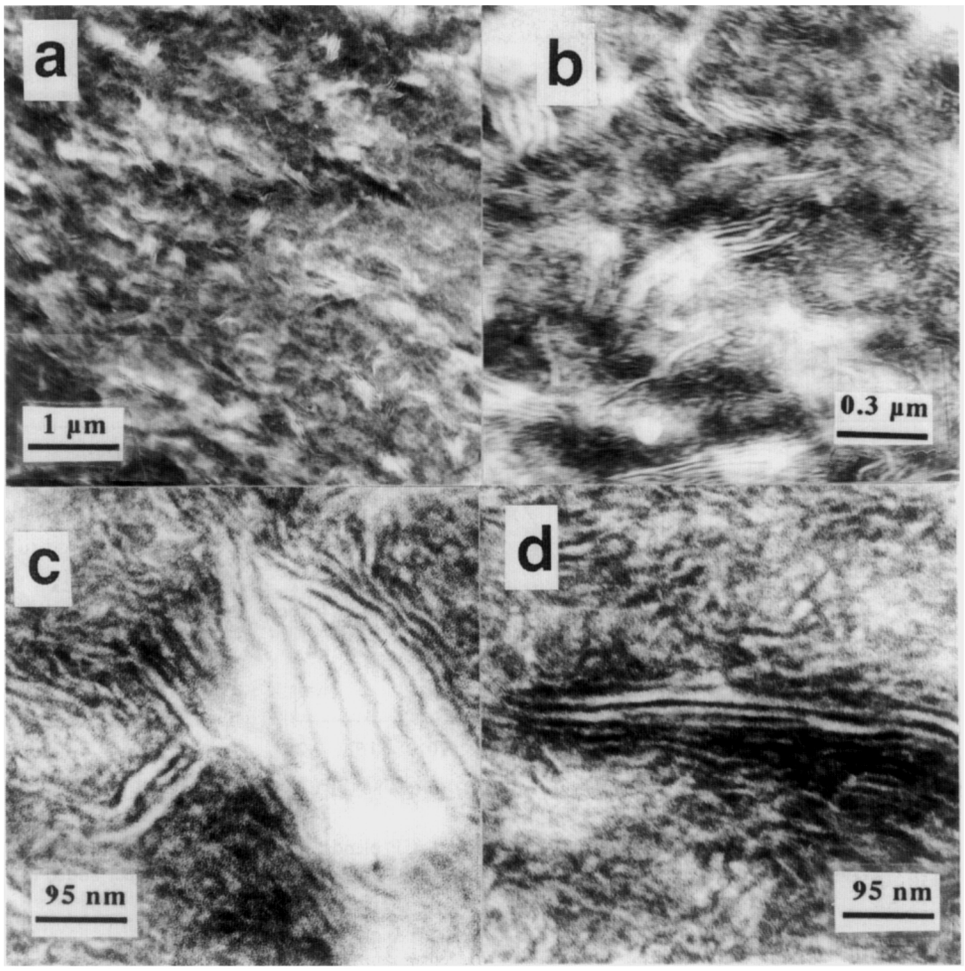

Figure 9 Transmission electron micrographs for cast films of LCP copolymer (F5) seen at different levels of magnification: (a) 8200×; (b) 37 500×; (c) 105 000×; (d) 105 000×. L phase (dark area) was selectively stained with ruthenium tetroxide. See *Table 1* for sample identification

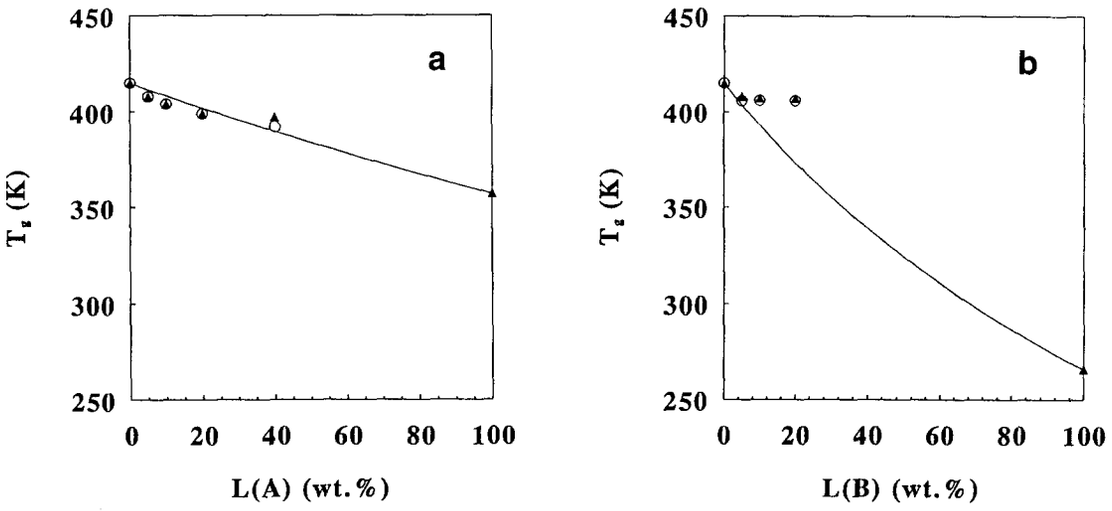

Figure 10 Glass transition temperature for L/CP blends with and without added LCP copolymer: (a) L(A)/CP blends without copolymer (▲) and with 5% copolymer added (○); (b) L(B)/CP blends without copolymer (▲) and with 5% copolymer added (○). The relationship according to the Fox equation[17] is given as a full curve

rising lignin component, and with and without LCP copolymer addition (constant 5% w/w). The copolymer had constant composition and M_n (i.e. 26 100).

The results of thermal analysis by d.m.t.a. revealed that the T_g of the amorphous CP component declined as L content rose in approximate accordance with the rule of mixing[17] (*Figure 10*). This T_g reduction was insensitive to the presence of LCP copolymer until the L content reached 40% (*Figure 10a*). At 40% L content, the T_g of the amorphous CP component in the blend revealed

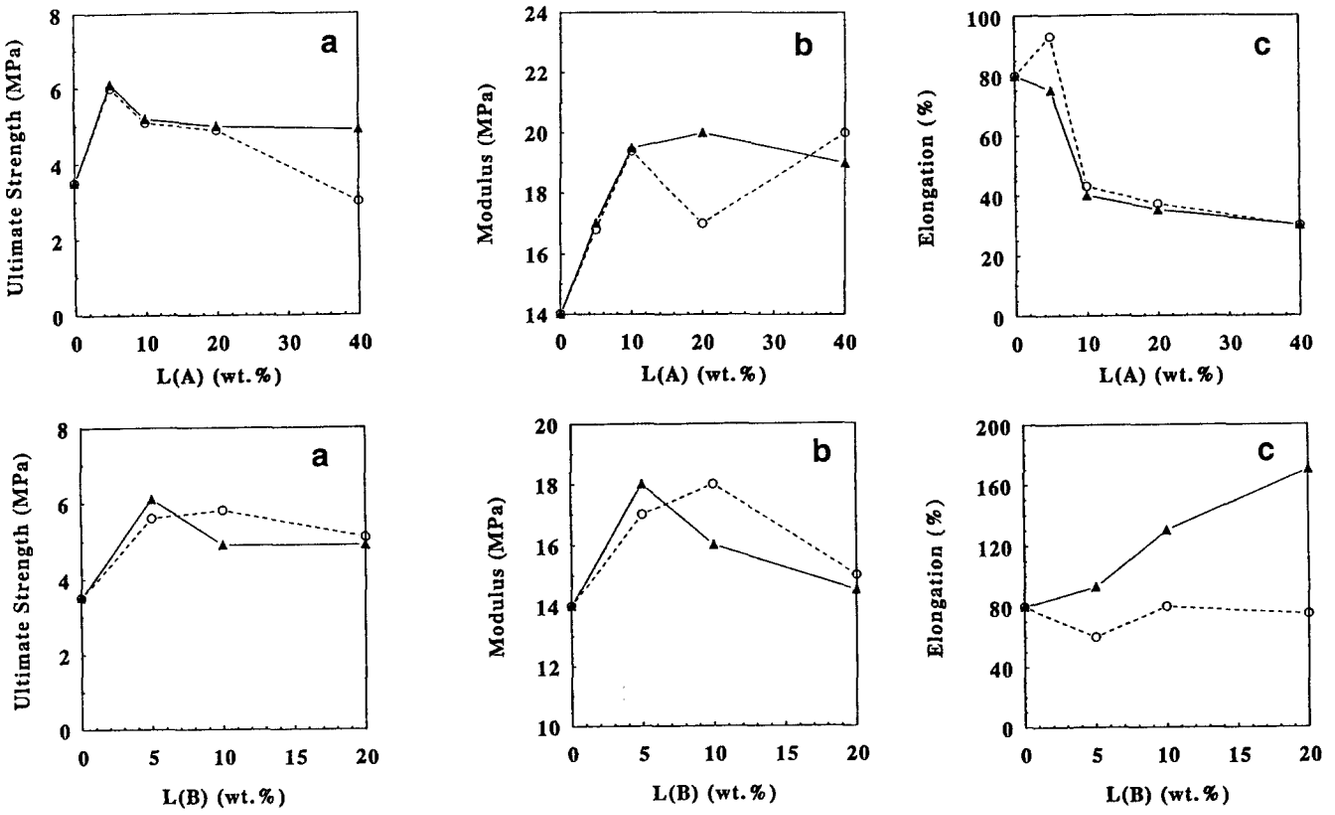

Figure 11 (a) Ultimate strength, (b) modulus and (c) elongation at break of L/CP blends: top row, L(A)/CP blends without copolymer (▲) and with 5% copolymer added (○); and bottom row, L(B)/CP blends without copolymer (▲) and with 5% copolymer added (○)

slightly greater compatibility between L and CP when copolymer was present (*Figure 10a*).

The blends of CP with low-T_g L revealed a similar phase compatibility between amorphous CP and L component only to a L content of 5% (*Figure 10b*). Above 5%, the T_g was independent of composition. Regardless of composition, the T_g of the amorphous CP component remained virtually insensitive to the presence of copolymer as was indicated by T_g. The fact that all T_g values varied (slightly) with L content suggests a (limited) degree of compatibility between CP and L, and this varied with the nature of the L. L with higher lignin content, L(A), appeared to remain more compatible with amorphous CP than highly propoxylated L (L(B)). The addition of LCP block copolymer did not seem to enhance further the compatibility between CP and either L component. The fact that CP and L have some degree of compatibility, and that this compatibility decreases when the propylene oxide content of the L component rises, is consistent with earlier observations[18].

The tensile properties of L/CP blends with and without LCP copolymer indicated that L contributes beneficially to the ultimate strength, modulus and elongation properties of CP; and that the addition of LCP copolymer fails to result in additional improvements (*Figure 11*). Ultimate strength for both CP blends, with L with T_g above or below room temperature, revealed a nearly 50% increase with 5% L content. This increase declined, slightly or significantly, as L content rose to 20 to 40% (*Figure 11a*).

Modulus data (*Figure 11b*) increased likewise, by 25 to 50%, as L content rose to 5 or 10%. This rise was more pronounced with L of T_g above room temperature. The modulus remained high with high-T_g L, and it declined with low-T_g L component (*Figure 11b*).

Elongation properties increased, remained constant, or decreased with L content depending on L type and amount (*Figure 11c*). Low-T_g L resulted in a gradual increase in elongation in the absence of copolymer; and elongation was constant when copolymer was present. High-T_g L had no significant effect on elongation at L contents of 5%, and it resulted in significant decreases at L contents of 10% or more. The presence of copolymer was ineffectual on elongation properties of blends with high-T_g L.

The reason why the blends with low-T_g L(B) were 'tougher' than those with high-T_g L(A) may be attributed to the nature of L(B). This material was rubbery at room temperature. The incorporation of rubber particles into the matrix of brittle CP tends to improve the impact resistance of the system. When the blend was modified by the addition of 5 wt% copolymer, the microcrystalline LCP domains served as particulate reinforcements; they strengthened the matrix and, for this reason, caused a significant increase in tensile strength.

CONCLUSIONS

Block copolymers consisting of L and CP had properties that varied with composition. CP segment size seemed to affect critically such copolymer properties as intrinsic viscosity, MHS exponential factor, crystallinity and T_m.

The solution properties of the copolymers suggested that these materials behave either like spheres or like rod-type molecules. The conformation was dictated by segment size.

Thermal analysis supported microphase separation between L and CP segments. CP segments crystallized, even at *DP* as low as 5. Degree of crystallinity reached its highest degree at CP chains of *DP* 60.

Copolymer morphologies exhibited a variety of features that ranged from disperse fibrils to spheres and ultimate lamella-type patterns in accordance with compositional and molecular-weight factors.

LCP block copolymers were unable to enhance significantly the thermal, mechanical, or morphological properties of physical blends between CP and L. This is attributed to the fact that CP and L form a partially miscible amorphous phase. Lignin content and T_g seemed to be more influential on eventual properties than the presence of phase-compatibilizing block copolymers.

ACKNOWLEDGEMENTS

Assistance with optical microscopy was provided by Dr A. Prasad, Department of Chemistry, and technical support with electron microscopy was provided by Mr Steven McCartney, Department of Materials Engineering, both VPI and SU. This assistance is acknowledged with gratitude. This study was financially supported, in part, by a grant from the National Science Foundation (Contract No. 85/12636).

REFERENCES

1 Ceresa, R. J. *Polymer* 1961, **2**, 213
2 Steinmann, H. W. *Polym. Prepr., Am. Chem. Soc. Div. Polym. Chem.* 1970, **11**, 285
3 Kim, S., Stannett, V. T. and Gilbert, R. D. *J. Polym. Sci., Polym. Lett. Edn.* 1973, **11**, 731
4 Kim, S., Stannett, V. T. and Gilbert, R. D. *J. Macromol. Sci. Chem. (A)* 1976, **10**, 671
5 Lee, K. S., Stannett, V. T. and Gilbert, R. D. *J. Polym. Sci., Polym. Chem. Edn.* 1982, **20**, 997
6 McBurney, L. F. in 'Cellulose' (Eds. E. Ott, H. M. Spurlin and M. W. Grafflin), 'High Polymers', Vol. V, Part I, Interscience, New York, 1954
7 Feger, C. and Cantow, H.-J. *Polym. Bull.* 1980, **3**, 407
8 Mezger, T. and Cantow, H.-J. *Angew. Makromol. Chem.* 1983, **116**, 13
9 de Oliveira, W. and Glasser, W. G. *Cellulose* in press
10 Kelley, S. S., Glasser, W. G. and Ward, T. C. *J. Wood Chem. Technol.* 1988, **8**(3), 341
11 Kelley, S. S., Glasser, W. G. and Ward, T. C. *J. Appl. Polym. Sci.* 1988, **36**, 759
12 Siochi, E. J., Ward, T. C., Haney, M. A. and Mahn, B. *Macromolecules* 1990, **23**, 1420
13 Glasser, W. G., Knudsen, J. S. and Chang, C. *J. Wood Chem. Technol.* 1988, **8**(2), 221
14 de Oliveira, W. Ph.D. Dissertation, Virginia Tech, Blacksburg, 1991
15 de Oliveira, W. and Glasser, W. G. *Macromolecules* 1994, **27**, 5
16 Buleon, A. and Chanzy, H. *J. Polym. Sci., Polym. Phys. Edn.* 1978, **16**, 383
17 Fox, T. G. *Bull. Am. Phys. Soc.* 1956, **2**(2), 123
18 Rials, T. G. and Glasser, W. G. *Wood Fiber Sci.* 1989, **21**(1), 80